C (1)-Symmetric cyclopentadienyl/indenyl-metallocene catalysts: synthesis, structure, isospecific polymerization of propylene and stereocontrol mechanism

Dimitra Theodosopoulou, Miguel Alonso de La Peña, Sary Abou Derhamine, Iskander Douair, Thierry Roisnel, Marie Cordier, Lorenzo Piola, Álvaro Fernández-Llamazares, Alexandre Welle, Laurent Maron, et al.

C_1-Symmetric {Cyclopentadienyl/Indenyl}-Metallocene Catalysts: Synthesis, Structure, Isospecific Polymerization of Propylene and Stereocontrol Mechanism

Dimitra Theodosopoulou,[a] Miguel Alonso De La Pena,[a] Sary Abou Derhamine,[a] Iskander Douair,[b] Thierry Roisnel,[c] Marie Cordier,[c] Lorenzo Piola,[d] Alvaro Fernandez,[d] Alexandre Welle,[d] Laurent Maron,[b] Jean-François Carpentier[a,*] and Evgueni Kirillov[a,*]

[a] Univ Rennes, CNRS, Institut des Sciences Chimiques de Rennes (ISCR), UMR 6226, F-35042 Rennes, France

[b] Univ Toulouse, INSA, UPS and CNRS, LPCNO, UMR 5215, F-31077 Toulouse, France

[c] Centre de diffraction X, Univ Rennes, CNRS, ISCR, UMR 6226, F-35700 Rennes, France

[d] TotalEnergies, Zone Industrielle Feluy C, B-7181 Seneffe, Belgium

Graphical Abstract / For the Table of content entry

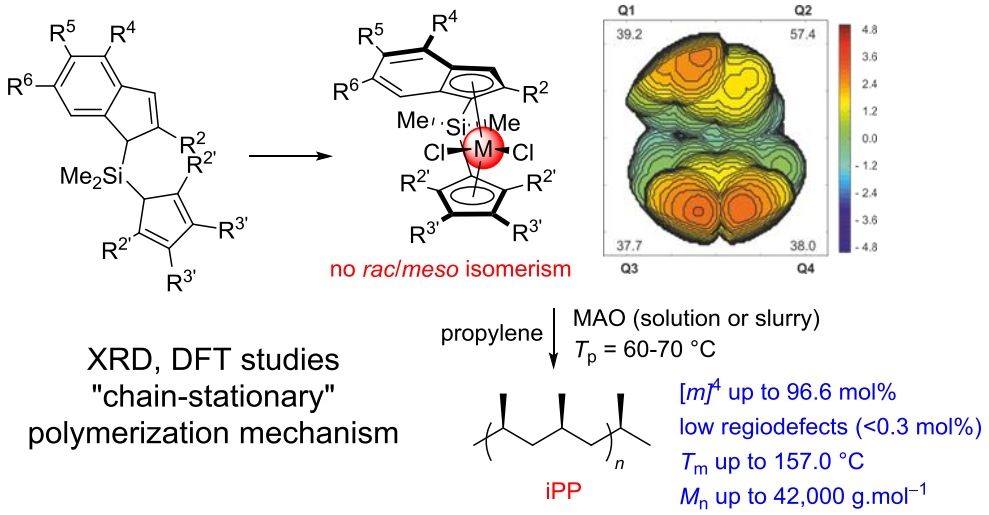

* Correspondence to Jean-François Carpentier (jean-francois.carpentier@univ-rennes.fr) and Evgueni Kirillov (evgueni.kirillov@univ-rennes.fr).

ABSTRACT

A series of new Me_2Si-bridged cyclopentadiene/indene proligands {$Me_2Si(R^{2',5'}{}_2\text{-}R^{3',4'}{}_2\text{-Cp})(R^2,R^4,R^5,R^6\text{-Ind})H_2$} (**1a-j**) with various substitution both on the indene and cyclopentadiene moieties was prepared. The corresponding C_1-symmetric group 4 *ansa*-metallocene complexes (M = Zr, Hf), namely, {$Me_2Si(Me_4Cp)(Ind)$}$ZrCl_2$ (**2a-Zr**), {$Me_2Si(Me_4Cp)$(2-Me,4-Ph-Ind)}MCl_2 (**2b-M**), {$Me_2Si(Me_4Cp)$(2-Me,4-Ph,6-*t*Bu-Ind)}$ZrCl_2$ (**2c-Zr**), {$Me_2Si(Me_4Cp)$(2-Me,4-Ph,5-OMe,6-*t*Bu-Ind)}MCl_2 (**2d-M**), {$Me_2Si(Me_4Cp)$(2-R',4-(3',5'-*t*Bu_2,4'-OMe-C_6H_2),5-OMe,6-*t*Bu-Ind)}$ZrCl_2$, R' = Me (**2e-Zr**), R' = Et (**2f-Zr**), {Me_2Si(2,5-Ph_2-3,4-Me_2-Cp)(2-Me,4-(3',5'-*t*Bu_2,4'-OMe-C_6H_2),5-OMe,6-*t*Bu-Ind)}$ZrCl_2$ (**2g-Zr**), {$Me_2Si(Me_4Cp)$(2-Me,4-(3',6'-*t*Bu_2-carbazol-4'-yl)-Ind)}$ZrCl_2$ (**2h-Zr**), {Me_2Si(2,5-Me_2,3,4-*i*Pr_2-Cp)(2-Me,4-Ph-Ind)}$ZrCl_2$ **(2i-Zr),** {Me_2Si(2,5-Me_2,3,4-*i*Pr_2-Cp)(2-Me,4-Ph,6-*t*Bu-Ind)}$ZrCl_2$ (**2j-Zr)** and {$Me_2Si(Me_4Cp)$(2-Me-4,5-[*a*]anthacene-Ind)}MCl_2 (**3k-Zr**) were synthesized and characterized by NMR spectroscopy and mass spectrometry. The solid-state molecular structures of **2b-Zr**, **2d-Zr**, **2e-Zr**, **2f-Zr**, **2j-Zr** and **2k-Zr** were determined by X-ray crystallography. The zirconocene complexes, once activated with MAO in toluene solution, exhibited propylene polymerization activities at 60 °C up to 161 000 kg(PP).mol(Zr)$^{-1}$.h^{-1}, affording highly isotactic polypropylenes (*i*PP) with [*m*]^4 up to 96.5% and T_m up to 157 °C. Also, metallocene complexes **2b**–**e-Zr** were supported on SiO_2-MAO and evaluated in slurry bulk propylene polymerization at 70 °C, producing *i*PPs with [*m*]^4 = 91.7–96.6 mol% and low regiodefects (0.2–0.3 mol%) contents, with productivities up to 636,000 kg(PP).mol(Zr)$^{-1}$.h^{-1}. DFT calculations allowed rationalizing a polymerization reaction mechanism occurring through "chain-stationary" enchainment with preference for 1,2- insertions.

INTRODUCTION

The development of well-defined catalysts for stereoselective polymerization of α-olefins ranks as one of the most prominent achievements of organometallic chemistry over the last decades. Thanks to pioneering contributions by Brintzinger, Kaminsky and others,[1,2,3,4] the first 'single-site' metallocene catalysts to produce highly isotactic polypropylene (*i*PP) were discovered. Two main families of group 4 metallocene precatalysts have emerged for isoselective propylene polymerization:[1,5] (*i*) C_2-symmetric *rac*-silylene-bridged *ansa*-bis(indenyl) complexes ({R_2Si-(Ind)$_2$}, hereafter referred to as {SBI}, **I**, Scheme 1)[6] and (*ii*) C_1-symmetric one-carbon-bridged cyclopentadienyl-fluorenyl ({R_2C-(Cp)(Flu)}, aka {Cp/Flu}, **II**)[7] complexes.

For the *rac*-{SBI}-systems, it has been demonstrated that both the rigidity of the catalyst backbone and the presence of a bulky 4-indenyl substituent are necessary for delivering high catalytic performance and stability at high-temperature.[8,9,10] The concept of *ultrarigidity* has been introduced by Rieger *et al.*[11] with the 7-OMe- and 4,4'-Ph- substitution in the indenyl fragments. The introduction of electron-donating substituents has also been shown to improve the stereoselectivity at high polymerization temperatures. For example, metallocene system *rac*-{Me_2Si(2-Me,4-Ph,5-OMe,6-*t*Bu-Ind)}$ZrCl_2$, in which the 4-Ph- and 5-OMe-indenyl substituents are presumed to stabilize the cationic catalytic intermediate, showed high activity and high stereoselectivity in the (co)polymerization of propylene.[12] Recently, another breakthrough in the design of metallocene polymerization catalyst systems that afford superior performances at very high temperatures has been achieved with a zirconocene incorporating conformationally rigid triptycenyl substituents.[13]

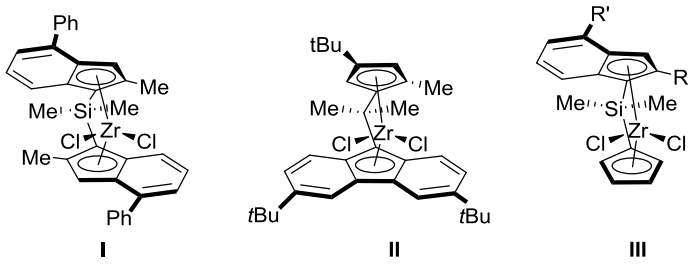

Scheme 1. Highly isoselective zirconocene precursors for propylene polymerization.

To a lesser extent, some research has been directed towards close isoselective analogues: C_1-symmetric cyclopentadienyl/indenyl (or {Cp/Ind}) metallocene systems (**III**). For instance, upon breaking the C_2-symmetry in the parent *rac*-{$Me_2Si(Ind)_2$}$ZrCl_2$ *via* replacement of one indenyl moiety with a cyclopentadienyl moiety, Spaleck *et al.*[14] obtained the metallocene {$Me_2Si(Cp)(Ind)$}$ZrCl_2$ which proved highly isoselective; the latter system features, however, lower activity and stereospecificity (represented by the average isotactic block length) (n_{iso} = 4.6) as compared to the parent bis(indenyl) analogue (n_{iso} = 50.1). C_1-Symmetric metallocenes are advantageous from the synthetic point of view, as no *rac*/*meso* isomerism exists for this family of complexes which exist in a single, isoselective form. Chien *et al.* have introduced the first C_1-symmetric one-carbon-bridged complex {$MeHC(C_5Me_4)(Ind)$}$TiCl_2$, which produces thermoplastic elastomeric polypropylenes (TPEs) having alternating isotactic-atactic stereoblock microstructures.[15] Collins *et al.* have reported similar R_2C- and R_2Si-bridged zircono- and hafnocene catalytic systems with no substituents on the Cp-ring that give elastomeric *i*PP ([*m*]^4 up to 54%).[16] Miyake's catalyst, {$Me_2C(3$-*t*Bu-$C_5H_3)(3$-*t*Bu-Ind)$}ZrCl_2$, produced iPPs ([*m*]^4 up to 98.8%) with high melting temperature (T_m up to 159 °C).[17] The C_1-symmetric complexes {$Me_2Si(Me_4Cp)(2$-R-Ind)$}MCl_2$ (R = H, Me; M = Ti, Zr) prepared by Do *et al.*[18] also exhibit good activity and provide moderate to highly isotactic PPs ([*m*]^4 up to 82%). With a good electron-donating

ability, the $CpMe_4$ moiety present in the aforementioned systems is expected to enhance the thermal stability of the metallocene catalysts as well as their solubility, and crystallizability.[19]

In this study, we aimed at developing new Si-bridged {Cp/Ind} proligands and related *ansa*-metallocene complexes of the type **III** (Scheme 1) to assess the influence of bulkier substitution patterns on the production of *i*PP. The catalytic performances of the metallocene complexes were, after their activation, investigated in homogeneous as well as heterogeneous (slurry) polymerization of propylene and compared to those of the classic catalytic system based on *rac*-{Me_2Si(2-Me,4-Ph-Ind)}$ZrCl_2$ (**I**). We also strove to rationalize the regio- and stereocontrol mechanism of the highly isoselective polymerization of propylene with the prepared {Cp/Ind}-metallocene systems. While for isoselective C_2-symmetric {SBI}-metallocene system **I** the chain-migratory insertion (CMI) mechanism has been identified,[20] for the C_1-symmetric {Cp/Flu}- counterparts (**II**) the validity of the "chain-stationary" insertion mechanism (*i.e.*, site epimerization by "back-skip") has been demonstrated.[21] The mechanism of formation of isotactic sequences during polymerization of propylene with {Cp/Ind}-type systems was assessed by theoretical computations of the first, second and third insertion steps.

RESULTS AND DISCUSSION

Synthesis of Proligands and Complexes. In order to assess the stereo-electronic influence of the electron-donating OMe-, *t*Bu- and carbazolyl substituents on polymerization performance, a series of new Zr and Hf complexes was synthesized. For benchmarking purposes, two reference complexes, namely, **2a-Zr**[22,23] and **3b-Zr**[24] were used. The corresponding Me_2Si-bridged proligands, incorporating substituted indenyl and cyclopentadienyl moieties, were prepared using regular multi-step protocols and were

characterized by ^{1}H, ^{13}C NMR spectroscopy and ASAP mass-spectrometry (see Experimental Section, Figures S9–S23).

The corresponding zirconium and hafnium complexes were obtained using a regular salt metathesis protocol in Et_2O from MCl_4 and the ligand dianions, prepared *in situ* by addition of *n*-butyllithium (2 equiv) to the proligand (Scheme 2). After workup and a consecutive recrystallization step, analytically pure complexes **2a–k-M** were isolated, generally in good yields (Scheme 2), as yellow or orange solids.

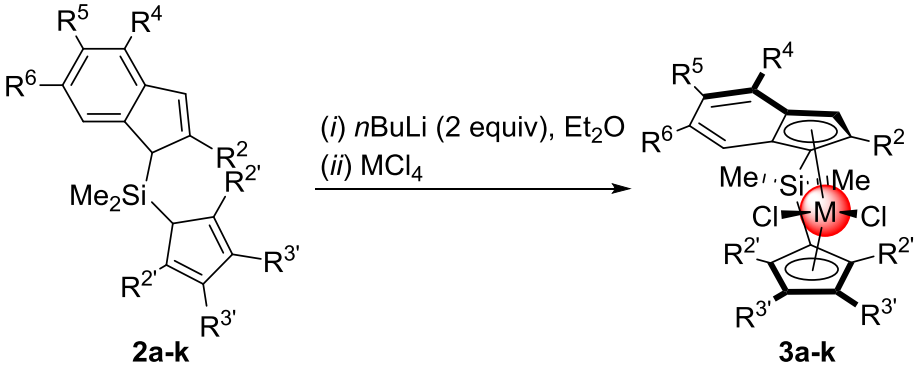

$R^{2'}$	$R^{3'}$	R^2	R^4	R^5	R^6	Proligand (Yield [%])	Complex (Yield [%])
Me	Me	H	H	H	H	**1a** (94)	**2a-Zr** (18)
		Me	Ph	H	H	**1b** (90)	**2b-Zr** (42) **2b-Hf** (30)
				H	*t*Bu	**1c** (94)	**2c-Zr** (45)
				OMe	*t*Bu	**1d** (91)	**2d-Zr** (50) **2d-Hf** (23)
			(3,5-*t*Bu$_2$,4-OMe)-Ph	OMe	*t*Bu	**1e** (98)	**2e-Zr** (30)
		Et	(3,5-*t*Bu$_2$,4-OMe)-Ph	OMe	*t*Bu	**1f** (84)	**2f-Zr** (23)
		Me	3,6-*t*Bu$_2$-carbazole	H	H	**1g** (82)	**2g-Zr** (10)
Ph			(3,5-*t*Bu$_2$,4-OMe)-Ph	OMe	*t*Bu	**1h** (94)	**2h-Zr** (34)
Me	*i*Pr		Ph	H	H	**1i** (42)	**2i-Zr** (38)
				H	*t*Bu	**1j** (54)	**2j-Zr** (5)
Me	Me	Me	triptycyl		H	**1k** (25)	**2k-Zr** (37)

Scheme 2. Synthesis of *ansa*-metallocenes **2a–k-M** (isolated yields of recrystallized complexes)

The solution structures of **2a–k-Zr** and **2a,d-Hf** were studied by ^{1}H and ^{13}C NMR spectroscopy and showed in each case a single set of resonances consistent with the C_1-symmetry of these species. Accurate assignment of the ^{1}H and ^{13}C NMR resonances (Figures S24–S47) was made by 2D HETCOR experiments. ASAP-HRMS mass-spectrometric analyses confirmed consistency of the compositions of all metallocene complexes.

Solid-State Structures of *ansa*-Metallocene Complexes. Single crystals of **2a,b,d,e,f,j,k-Zr** and **2b,d-Hf** suitable for X-ray crystallography were grown from toluene, toluene/heptane (1:3 *v/v*) or heptane solutions at room temperature. In the solid state, these metallocenes (Figures 1–7) exhibit geometrical parameters (Table 1) essentially similar to those observed for metallocene dichloride congeners incorporating R_2Si-bridged cyclopentadienyl and related ligands (*e.g.*, **I**).[6] All the C_1-symmetric complexes feature a planar chirality and their unit cells are composed of pairs of enantiomers. The coordination of the five-membered ring of the indenyl ligand in most complexes deviates slightly from η^5 towards a reduced η^3 mode, as revealed by the significant differences in the M–C(ring) distances (average of 0.12–0.23 Å) between the shortest and the longest bond lengths. Both the Zr–Ind_{cent} and Zr–Cp_{cent} distances are found in the relatively narrow respective ranges, 2.239(4)–2.256(4) and 2.213(5)–2.236(4) Å. Also, the Cp_{cent}–M–Ind_{cent} bite angles in the new *ansa*-metallocenes (range = 127.94–129.49 deg) do not differ significantly. The largest dihedral angles between the Cp-ring and Ind-ligand planes (61.78, 62.23 and 62.71 deg, respectively) are observed for complexes **2d-Hf**, **2a-Zr** and **2j-Zr**, while in **2e-Zr** and **2f-Zr**, those appeared to be somewhat smaller (60.61 and 60.99 deg, respectively); this is apparently due to the mutual repulsive interactions of the OMe- and *t*Bu- substituents. Also, the

geometrical parameters of the hafnium congeners **2b-Hf** and **2d-Hf** are comparable to those observed respectively in **2b-Zr** and **2d-Zr**, which is accounted for the similar size of these metal centers (ionic radius for six-coordinate metal centers, Hf^{4+}: 0.71 Å *vs*. Zr^{4+}: 0.72 Å).[25]

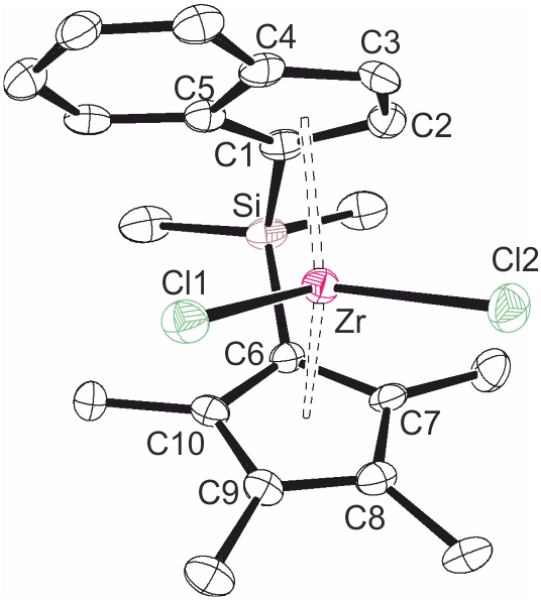

Figure 1. Molecular structure of **2a-Zr** (H atoms omitted for clarity; ellipsoids drawn at the 50% probability level).

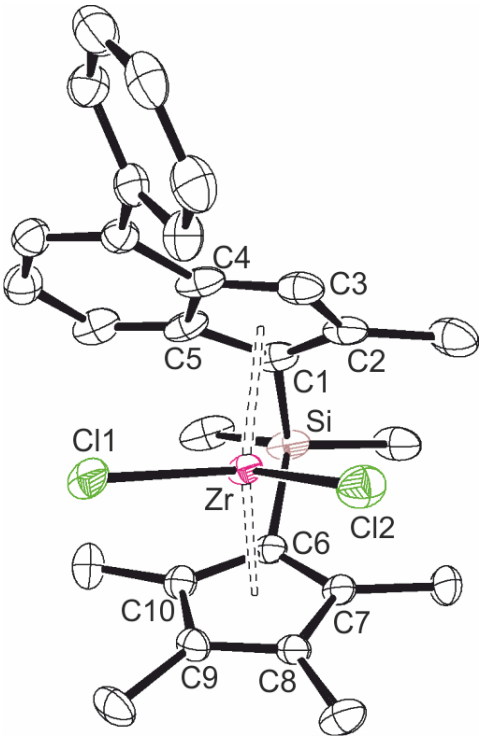

Figure 2. Molecular structure of **2b-Zr** (H atoms omitted for clarity; ellipsoids drawn at the 50% probability level).

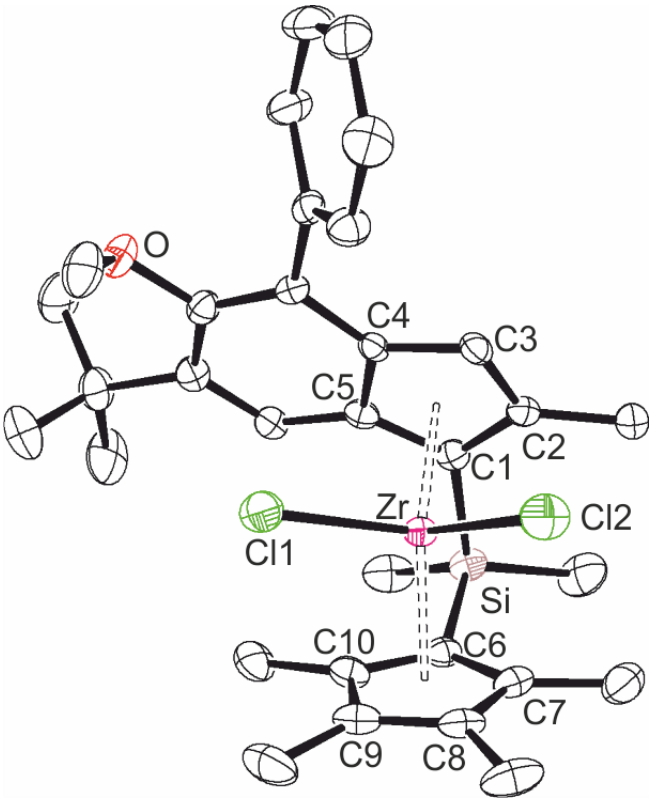

Figure 3. Molecular structure of **2d-Zr** (H atoms omitted for clarity; ellipsoids drawn at the 50% probability level).

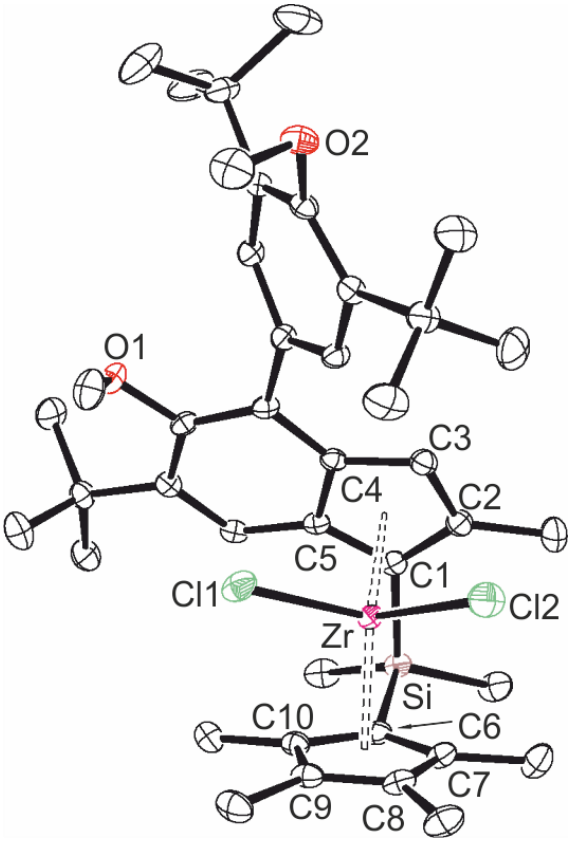

Figure 4. Molecular structure of **2e-Zr** (H atoms omitted for clarity; ellipsoids drawn at the 50% probability level).

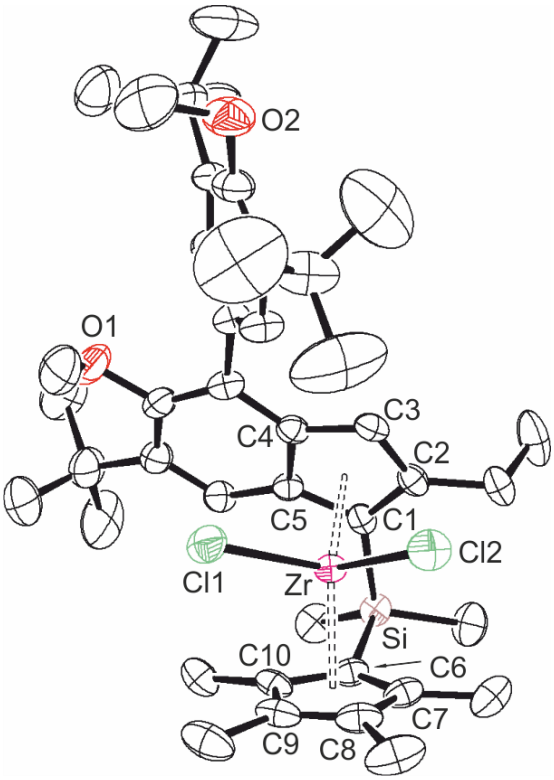

Figure 5. Molecular structure of **2f-Zr** (H atoms omitted for clarity; ellipsoids drawn at the 50% probability level).

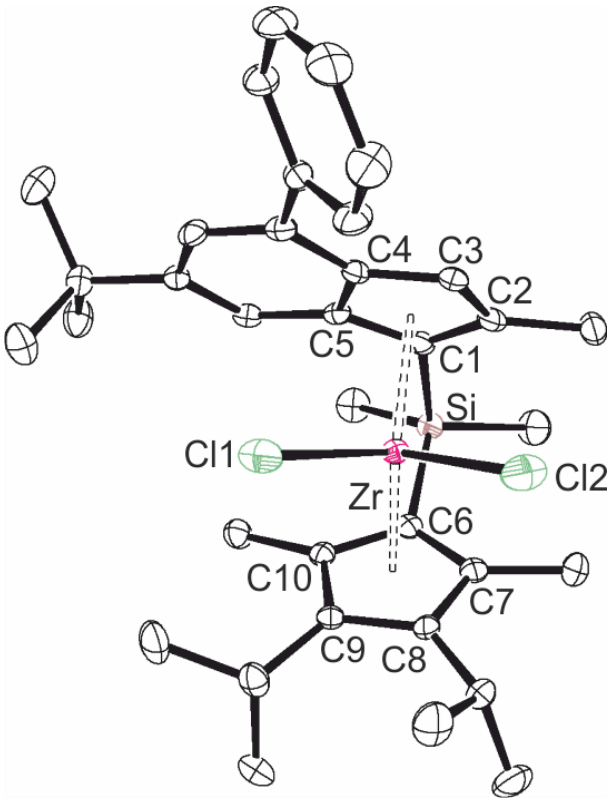

Figure 6. Molecular structure of **2j-Zr** (H atoms omitted for clarity; ellipsoids drawn at the 50% probability level).

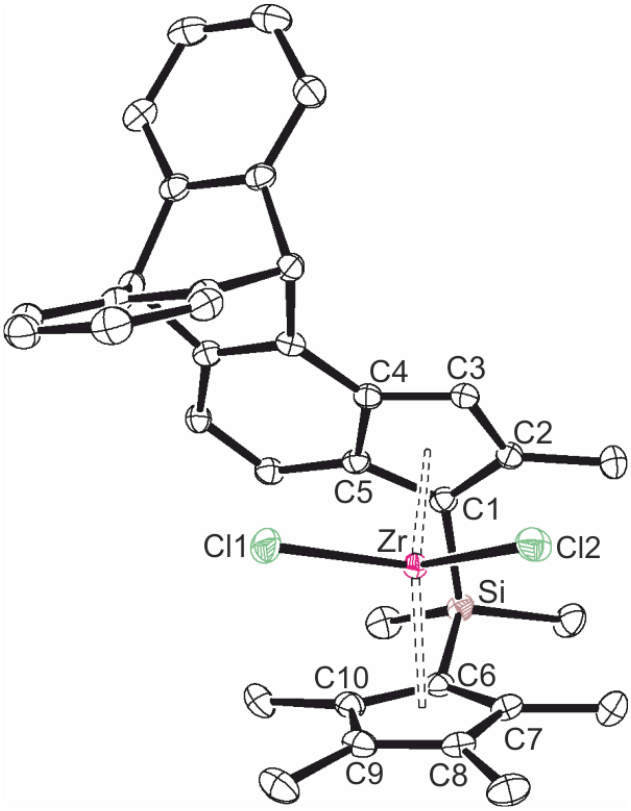

Figure 7. Molecular structure of **2k-Zr** (H atoms omitted for clarity; ellipsoids drawn at the 50% probability level).

Table 1. Selected bond distances (Å) and angles (deg) for metallocenes **2a,b**,**d,e,f,k-Zr** and **2b,d-Hf** and reference **I**.[6]

	I [6]	**2a-Zr**	**2b-Zr**	**2b-Hf**	**2d-Zr**	**2d-Hf**	**2e-Zr**	**2f-Zr**	**2j-Zr**	**2k-Zr**
M–Cl	2.419(1)	2.4189(16)	2.415(10)	2.386(15)	2.406(9)	2.417(10)	2.424(5)	2.444(2)	2.413(7)	2.4000(5)
		2.448(16)	2.436(11)	2.404(18)	2.441(8)	2.388(10)	2.439(6)	2.419 (2)	2.437(9)	2.4469(5)
M–C(l)	2.478(3)	2.486(5)	2.484(3)	2.461(4)	2.446(3)	2.460(4)	2.471(2)	2.465(5)	2.475(2)	2.4867(18)
M–C(2)	2.517(4)	2.471(6)	2.536(4)	2.508(4)	2.517(3)	2.548(4)	2.540(2)	2.503(5)	2.547(2)	2.5108(18)
M–C(3)	2.577(3)	2.574(6)	2.591(4)	2.597(4)	2.600(3)	2.582(4)	2.616(2)	2.586(5)	2.607(2)	2.5559(18)
M–C(4)	2.640(4)	2.676(5)	2.633(4)	2.606(4)	2.672(3)	2.655(4)	2.657(2)	2.670(4)	2.637(2)	2.6335(18)
M–C(5)	2.568(4)	2.580(5)	2.544(4)	2.523(4)	2.561(3)	2.500(4)	2.535(2)	2.566(5)	2.521(2)	2.5703(17)
M–Ind$_{cent}$	2.243(4)	2.251(5)	2.250(4)	2.234(4)	2.256(4)	2.239(4)	2.256(4)	2.251(4)	2.251(4)	2.243(5)
M–Cp$_{cent}$	-	2.213(5)	2.214(4)	2.201(4)	2.234(3)	2.214(4)	2.228(4)	2.236(4)	2.236(4)	2.218(5)
M–C(6)	-	2.465(5)	2.466(3)	2.430(4)	2.464(3)	2.449(4)	2.469(2)	2.464(6)	2.466(2)	2.4481(18)
M–C(7)	-	2.474(5)	2.501(4)	2.487(4)	2.494(3)	2.472(4)	2.497(2)	2.488(6)	2.470(2)	2.4874(18)
M–C(8)	-	2.582(5)	2.586(4)	2.575(4)	2.630(2)	2.607(4)	2.603(2)	2.612(6)	2.597(2)	2.6015(18)
M–C(9)	-	2.596(5)	2.578(3)	2.574(4)	2.612(3)	2.600(4)	2.617(2)	2.622(6)	2.656(2)	2.6105(18)
M–C(10)	-	2.494(6)	2.491(3)	2.485(4)	2.512(3)	2.492(4)	2.507(2)	2.528(5)	2.537(2)	2.4888(18)
Cp$_{cent}$–M–Ind$_{cent}$	128.5(3)	127.94(5)	128.71(4)	129.25(4)	128.85(2)	129.49(4)	128.81(2)	128.48(5)	128.26(4)	128.31(5)
Dihedral Angle*	59.2	62.23	60.54	60.57	60.57	61.78	60.61	60.99	62.71	61.01

*Dihedral angle between the planes of the Cp ring and the Ind moiety.

Propylene Polymerization Catalysis. The *ansa*-metallocene complexes **2a**–**j**-**M**, in combination with MAO, were first tested in homogeneous polymerization of propylene (Table 2).[26] For comparison purposes, the catalytic performance of the reference complex **I** was determined under identical conditions.

In terms of activity and productivity, the performances of the synthesized series of metallocene precursors are noteworthy and compare well with those of the reference complex **I** (entry 1, 53,300 kg(PP)·mol(Zr)$^{-1}$·h^{-1}). In the benchmark experiments with **2a**-**Zr**, the productivity (entry 2, 64,700 kg(PP)·mol(Zr)$^{-1}$·h^{-1}) was found to be similar to that of complex **I**. Regarding the other closer analogues **2b**-**Zr** and **2c**-**Zr** having the 4-Ph substitution, the former lacking the 6-*t*Bu substituent stood out for its high productivity (entry 3, 122,000 kg(PP)·mol(Zr)$^{-1}$·h^{-1}) compared to that of the latter (entry 5, 13,300 kg(PP)·mol(Zr)$^{-1}$·h^{-1}). The system based on **2g**-**Zr**/MAO (entry 11, 161,000 kg(PP)·mol(Zr)$^{-1}$·h^{-1}) outperformed the other synthesized metallocene catalysts; this can be plausibly accounted for by the high stability of the 4-*N*-carbazolyl-substituted zirconocenes as recently documented in literature.[27] Remarkably, the systems based on **2d**-**Zr**, **2e**-**Zr**, and **2f**-**Zr** also showed high productivities, which were significantly increased in the case of **2e**-**Zr** (entry 9, 103,000 kg(PP)·mol(Zr)$^{-1}$·h^{-1}). This result can be accounted for by the presence of the 5- and 4'-OMe- groups with the *t*Bu-groups on the neighboring positions of the indenyl moiety and the 4-Ph group, respectively. The much lower productivity of **2h**-**Zr** (entry 14, 9,200 kg(PP)·mol(Zr)$^{-1}$·h^{-1}), even at higher catalyst loading, could stem from both the electron-withdrawing properties and the bulkiness of the 2,5-Ph-substituents in the Cp ligand. On the other hand, the introduction of the two isopropyl groups in the frontal positions (3,4-) of the cyclopentadienyl ligands in **2i**-**Zr** and **2j**-**Zr** unexpectedly appeared to be deleterious for their performances (entries 15–20); only small amounts of oligomeric materials (M_n = 1,800 g·mol^{-1}) were isolated (entry 16). We surmise that this could be the result of intramolecular C–H activation reaction

between the proximal methyl groups of the *i*Pr substituents and Zr–alkyl function of the cationic complex, leading to the formation of rather stable zirconacyclic products as dormant species.[28]

The inactivity of hafnium complexes **2b-Hf** and **2d-Hf** is in striking contrast to their zirconium isostructural analogues **2b-Zr** and **2d-Zr**; this is not entirely unexpected and is in line with the so-called "hafnium-effect".[29,30,31] The latter is stipulated to arise from the somewhat more stable Hf−C σ-bond compared to the Zr−C bond (by ca. 5 kcal.mol^{-1}), which results in inherently lower chain propagation rate for hafnium complexes as well as by the slightly lower Lewis acidity of the hafnium metal center. In addition, the strong inhibiting effect in propylene polymerization of "free" $AlMe_3$ (TMA) derived from MAO has been evidenced for hafnocene catalysts in several cases.[32] As presumed, $AlMe_3$ binds hafnocenium cations much more strongly than the zirconium counterparts, eventually affording very stable and poorly active heterobimetallic Hf/Al species.

The polypropylenes derived from the C_1-symmetric complexes featured relatively narrow molecular weight distributions (M_w/M_n = 2.2–2.5) compatible with a single-site behavior. The molecular weights of the PPs produced with the systems based on **3b-Zr**, **3c-Zr**, **2d-Zr**, **2g-Zr**, **2h-Zr** and **2k-Zr** were within a narrow range, M_n = 21.6–30.9 kg.mol^{-1}, while those of the polypropylenes obtained with systems **2e-Zr** and **2f-Zr** were slightly increased (M_n = 41.9 and 39.9 kg.mol^{-1}, respectively).

All the above complexes yielded highly isotactic polypropylenes with contents of $[m]^4$ pentads ranging from 91.8 (**2b-Zr**) to 93.1–96.5% (**2d-Zr**, **2e-Zr**, **2f-Zr** and **2k-Zr**, respectively), depending on the substituents on the indenyl ligand. The incorporation of an additional 4'-OMe substituent on the 4-Ph group of the indenyl in **2e-Zr** has a clear beneficial effect on the stereoselectivity ($[m]^4$ = 96.5%, entry 9). The regioselectivities for primary insertion of the monomer (99.6–99.9 %) were nearly perfect for all metallocene systems.

Since the amount of regioerrors in polymers was found similar for entries 3, 5, 6, 9 and 21, the observed variation of the melting temperature is apparently influenced directly by the amounts of stereodefects. Hence, the T_m of *i*PPs produced with **2e-Zr**, **2f-Zr** and **2k-Zr** (157.0, 156.9 and 157.0 °C, respectively) is in line with the highest stereospecificities observed within the whole prepared series of metallocene (pre)catalysts and can be ascribed to the presence of an additional electron-donating substituent on the rigid catalyst backbone.[33] However, it was quite an unexpected result that the oligomers produced with **2i-Zr** complex were completely atactic, as shown by $^{13}C\{^1H\}$ NMR spectroscopy (Figure S53). The ratio between vinylidene, vinyl and isobutenyl chain-ends in these oligomers was estimated by ^1H NMR spectroscopy (Figure S54) to be of 93:6:1, respectively; this is diagnostic of β-H elimination/transfer-to-monomer after a primary (1,2-) insertion as the principal termination mechanism.

Table 2. Homogeneous Isoselective Propylene Polymerization [a]

entry	Precat	$[M]_0$ [μmol·L^{-1}]	[Al]/[Zr]	T_{polym} [°C][b]	m_{iPP} [g]	Productivity [kg·mol^{-1}·h^{-1}]	T_m [°C][c]	T_{cryst} [°C][c]	M_n [kg·mol^{-1}][d]	M_w/M_n [d]	$[m]^4$ [%][e]	2,1 ins [%][e]	*i*Butyl chain ends [%][e]
1	**I**	2.0	2 500	60 (65)	8.0	53,300	152.2	124.7	132.1	3.1	93.4	0.4	0.0
2	**2a-Zr**	2.0	5 000	60(63)	9.7	64,700	119.5	89.0	9.1	2.0	71.7	0.2	0.1
3	**2b-Zr**	2.0	5 000	60(66)	18.3	122,000	149.0	112.0	25.2	2.3	91.8	0.1	0.2
4	**2b-Hf**	10.0	5 000	60 (63)	0.0	0	-	-	-	-	-	-	-
5	**2c-Zr**	2.0	5 000	60(64)	3.0	13,300	145.0	107.5	26.6	2.5	90.5	0.3	0.2
6	**2d-Zr**	2.0	5 000	60 (65)	7.6	50,500	151.7	114.0	29.2	2.2	94.3	0.2	0.2
7	**2d-Hf**	10.0	5 000	60 (63)	0.0	0	-	-	-	-	-	-	-
8	**2e-Zr**	3.0	2 500	60 (72)	18.0	80,000	155.2	113.7	34.9	2.2	97.2	0.2	<0.1
9		2.0	5 000	60(66)	15.5	103,000	157.0	118.0	41.9	2.2	96.5	0.2	0.1
10	**2f-Zr**	2.0	5 000	60 (65)	9.3	62,000	155.9	114.3	39.9	2.4	94.4	0.4	0.1
11	**2g-Zr**	2.0	5 000	60 (74)	24.1	161,000	149.2	111.8	n.d.	n.d.	n.d.	n.d.	n.d.
12		1.5	5 000	60 (66)	11.5	102,000	151.7	111.6	25.0	2.2	93.6	0.0	0.1
13	**2h-Zr**	2.0	5 000	60 (64)	0.0	0	-	-	-	-	-	-	-
14		10.0	5 000	60 (64)	6.9	9,200	153.5	115.1	21.6	2.3	93.1	0.0	0.2
15	**2i-Zr**	2.0	5 000	60(62)	0.0	0.0	-	-	-	-	-	-	-
16		10.0	5 000	60(64)	1.4 (oil)	9,340	n.o.	n.o.	1.8	1.3	n.d.	n.d.	n.d.
17		10.0	1 000[f]	60(63)	<0.1 (oil)	0.0	-	-	-	-	-	-	-
18	**2j-Zr**	2.0	5 000	60(60)	0.0	0.0	-	-	-	-	-	-	-

19[g]		10.0	10 000	60(60)	0.8 (oil)	5,300	n.o.	n.o.	n.d.	n.d.	n.d.	n.d.	n.d.
20[h]		10.0	5 000	60(60)	0.6 (oil)	3,900	n.o.	n.o.	n.d.	n.d.	n.d.	n.d.	n.d.
21	**2k-Zr**	2.0	5 000	60 (64)	7.1	47,000	157.0	118.0	30.9	2.3	95.0	0.1	0.1

[a] Polymerization conditions: 300 mL-high pressure glass reactor equipped with a Pelton turbine; Solvent: toluene, 150 mL; P(propylene) = 5 bar; time = 30 min; n.o. = not observed; n.d. = not determined. [b] Data in brackets refer to the maximum temperature reached in the reactor. [c] Determined by DSC from second run. [d] Determined by GPC analysis vs polystyrene standards. [e] Determined by ^{13}C NMR spectroscopy. [f] TIBAL/$[Ph_3C]^+[B(C_6F_5)_4]^-$ (200:1 [g] Polymerization time = 60 min. [h] Pre-activation with MAO (5 000 equiv vs [Zr]) for 1 h and TIBAL (5 000 equiv vs [Zr]) as scavenger.

The SiO_2-MAO-supported versions of **2b**–**e-Zr** (***supp*-2b**–**e-Zr**) were evaluated under slurry conditions in propylene homopolymerization (Table 3). In line with previous results,[34] the productivity of the supported metallocene *supp*-**2b-Zr** appeared to be somewhat lower as compared to its homogeneous version, (entry 1, 76,000 vs 122,000 kg(PP)·mol(Zr)$^{-1}$·h^{-1}). The supported metallocenes displayed higher productivities when an OMe group (*supp*-**2e-Zr**) and noticeably two OMe groups (*supp*-**2e-Zr)** were grafted on the indenyl ligand framework. The most active supported metallocene system appeared to be *supp*-**2e-Zr** (entry 4, 636,000 kg(PP)·mol(Zr)$^{-1}$·h^{-1}), consistent with the trend observed for the homogeneous version. In the series of the supported metallocene catalysts, the highest molecular weight polymer (that is, the lowest MI2 value; see Table 3, footnote *d*) was obtained with *supp*-**2b-Zr** (entry 1), whereas *supp*-**2c-Zr** afforded the lowest molecular weight polymer on the MI2 scale (entry 2). Also, all produced *i*PPs exhibited a low content of regiodefects (0.2–0.3%) and a high [*m*]^4 content (91.7–96.6%). The different amounts of stereodefects have an impact on the T_m, which is reflected by the highest value of 155.2 °C for the *i*PP obtained with *supp*-**2e-Zr**, which is comparable to the value for the polymer obtained with the homogeneous version **2e-Zr** (156.9 °C).

Table 3. Heterogeneous propylene polymerization. [a]

Entry	Catalyst composition	m_{iPP} [g]	Productivity [kg·mol^{-1}·h^{-1}]	T_m [°C][b]	T_c [°C][b]	[*m*]^4 [%][c]	2,1-ins [%][c]	MI2 [g/10 min]
1	*supp*-**2b-Zr**	182	76,000	147.8	109.0	91.9	0.2	35
2	*supp*-**2c-Zr**	262	114,000	144.5	104.0	91.7	0.3	144.6
3	*supp*-**2d-Zr**	418	192,000	150.7	107.0	95.4	0.3	79
4	*supp*-**2e-Zr**	1045	636,000	155.2	109.0	96.6	0.2	65.2

[a] Polymerization conditions: 8L reactor; catalyst introduced = 120 mg; propylene = 4.5 L; time = 60 min; temperature = 70 °C; scavenger = TIBAL; 0.5 NL H_2. [b] Determined by DSC from second run. [c] Determined by ^{13}C NMR spectroscopy. [d] The Melt Flow Index (MI2) is defined as the number of grams of polymer extruded in ten minutes as measured by ASTM Method D 1238.

Theoretical studies on the stereocontrol mechanism with C_1-symmetric {Cp/Ind}-metallocene systems. In parallel we aimed at rationalizing the mechanism of formation of isotactic sequences during propylene polymerization with these {Cp/Ind} systems by DFT computations of the first, second and third insertion steps.[21] Energetic data for the three consecutive propylene insertion steps from the cationic precursors [{$Me_2Si(Me_4Cp)$(2-Me,4-Ph,6-*t*Bu-Ind)}ZrMe]$^+$ (**[2c-Zr-Me]$^+$**) and [{$Me_2Si(Me_4Cp)$(2-Me,4-Ph,5-OMe,6-*t*Bu-Ind)}ZrMe]$^+$ (**[2d-Zr-Me]$^+$**) were calculated. We considered at each insertion step the formation of the corresponding propylene π-adducts *via* eight different possible pathways, namely 1,2- (primary, *pr*) and 2,1- (secondary, *sec*) insertions for the two different enantiofaces, *re* and *si*, for both a migratory and stationary propagation (Schemes S1–9). The main features of this study are summarized in Table S3. For each insertion step, the zero of energy corresponds to the *anti* isomer of the bare cation (that is more stable than the *syn* isomer by 1.7–1.9 kcal·mol^{-1} for the very first insertion step) and a propylene molecule on an infinite distance (Scheme 3).

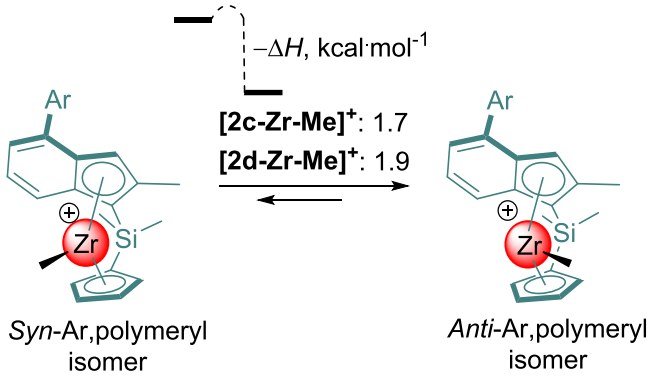

Scheme 3. Epimerization (back-skip) process for C_1-symmetric {Cp/Ind} metallocene catalysts.

Based on our computational results, we suggest that, similarly to the C_1-symmetric {Cp/Flu}-type catalysts,[21b] propylene polymerization with these {Cp/Ind} analogues also

operates through a stationary mechanism with a sequence of 1,2- (primary) insertions systematically occurring from a more crowded and a more stereoselective side, yielding an isotactic chain (Scheme 4).

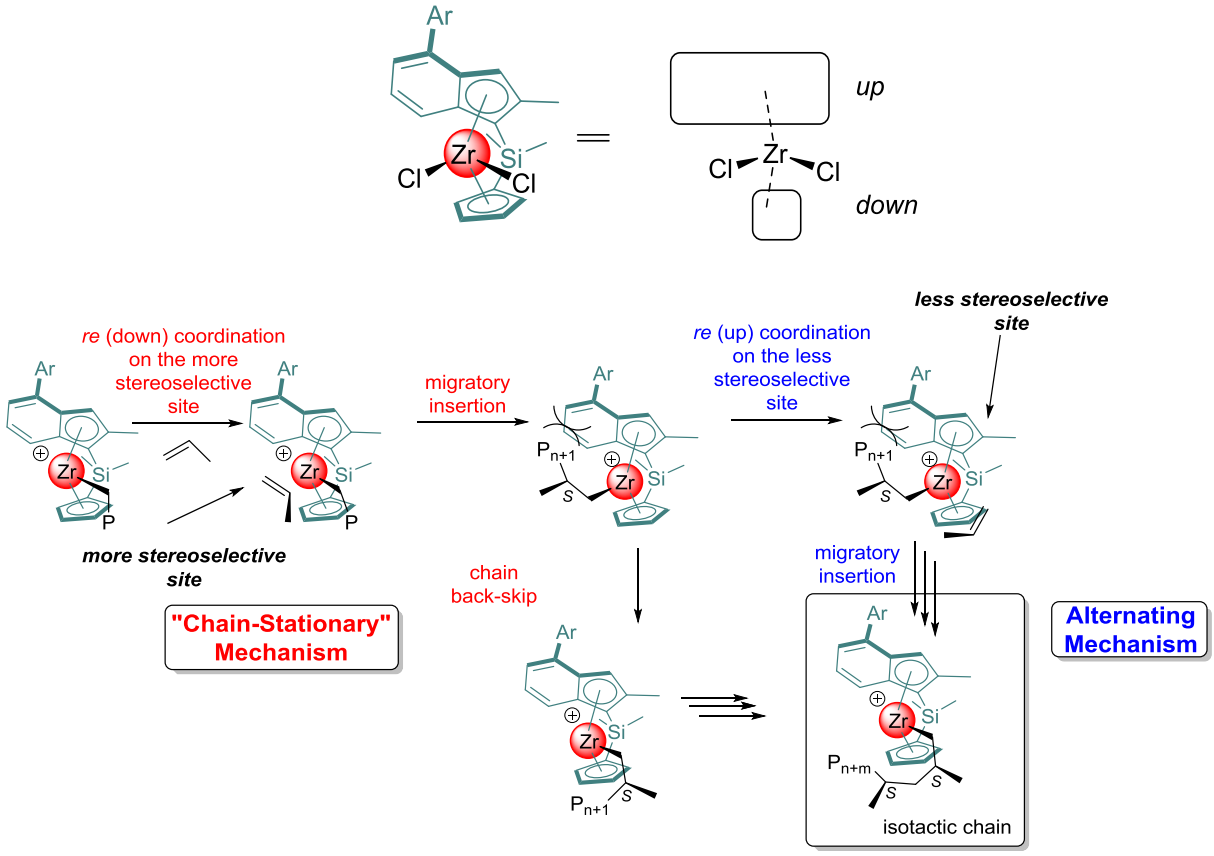

Scheme 4. Proposed competing stereocontrol mechanisms with C_1-symmetric {Cp/Ind}-metallocene catalysts (P stands for polymeryl chain).

Table 4. Relative energetic data (kcal·mol^{-1}) calculated for the three first propylene insertion steps with systems **[2c,d-Zr-Me]$^+$**.

[2c-Zr-Me]$^+$	1s^t insertion: *down*	2nd insertion: *down*	3^d insertion: *down*
Mechanism		*Stationary*	
Lowest barrier $\Delta H^{\neq}$	11.4	7.2	7.0
Insertion energy $\Delta_r H$	–15.6	–18.8	–22.4
%(2,1-) *experimental*		0.2–0.3	
[2d-Zr-Me]$^+$	1s^t insertion: *down*	2nd insertion: *down*	3^d insertion: *down*
Mechanism		*Stationary*	
Lowest barrier $\Delta H^{\neq}$	12.7	5.8	6.3
Insertion energy $\Delta_r H$	–13.7	–19.5	–20.0
%(2,1-) *experimental*		0.2–0.3	

As can be seen from the results summarized in Table 4, there is a reasonable kinetic preference (the differences lye within the precision of the DFT method) and a clear thermodynamic preference for the 1,2-insertion at the crowded (stereoselective) site in **[2c-Zr-Me]$^+$**. Indeed, the associated barriers are relatively low (maximum of 11.4 kcal·mol^{-1}) and each insertion is thermodynamically favorable (up to –22.4 kcal·mol^{-1} gain at the third insertion). It also appears that, for each insertion, the *down* orientation is favored, leading for a chain-stationary propagation to the formation of an isotactic polymer. The preference for the *down* orientation of propylene at the different insertion transition state is simply due to the reduced steric repulsion effect as the methyl substituent of propylene points in the opposite direction to the indenyl ligand (Scheme 4). The same computations were conducted for **[2d-Zr-Me]$^+$**, though only the two first insertion steps were probed in this case. Alike **[2c-Zr-Me]$^+$**, the propagation with **[2d-Zr-Me]$^+$** was calculated to be also stationary with a sequence of 1,2- insertions. The associated barriers are quite similar to those found for the other system (maximum of 12.7 kcal·mol^{-1} for the first insertion) and an important thermodynamic gain at each insertion (up to 19.5 kcal·mol^{-1} at the second insertion). Finally, the calculations

corroborated that the two catalysts should only give a very limited amount of 2,1- insertion, in line with the experimental observations.

The probabilistic descriptors *a*, *b* and *k*, calculated from the experimental pentad distributions (Table 5) using the three-parameter model for C_1-symmetric systems described by Farina *et al.*,[35] are in agreement with the isoselective behavior of the {Cp/Ind} metallocene systems and the computational model. For instance, the probability values of stereoselective insertion on the crowded metallocene face *b* are generally coherent with the relative sizes of the steric pockets expressed as $\Delta\%V_{free,Q1}$ of the corresponding quadrants Q1 representing the active site (Table S2, Figure S50). The probabilities of site epimerization, represented by the corresponding probabilistic descriptors *k*, characterizing the ability of the growing chain to reside preferably on the less crowded (and much less stereoselective) side, are comparable to those obtained for the related highly isoselective C_1-symmetric {Cp/Flu} systems.[21b] Yet, our attempts to unequivocally estimate descriptors *a*, *b* and *k* from the DFT-calculated data for **[2c,d-Zr-Me]**$^+$ and use them for theoretical prediction of the pentad distributions afforded overestimated $[m]^4$ values (>99%).

Table 5. Pentad distributions (%) and corresponding probability parameters[35] determined experimentally for **2a–h,k-Zr**, and those simulated using a three-parameter model.[21b]

	2a-Zr [a]		**2b-Zr** [a]		**2c-Zr** [a]		**2d-Zr** [a]		**2e-Zr** [b]		**2f-Zr** [b]		**2g-Zr** [b]		**2h-Zr** [b]		**2k-Zr** [b]	
	Exp	Calc	Exp	Calc	Exp	Calc	Exp	Calc	Exp	Calc	Exp	Calc	Exp	Calc	Exp	Calc	Exp	Calc
M_n [$\times 10^3$]	9.1	-	25.2	-	26.6	-	29.2	-	41.9	-	39.9	-	25.0	-	21.6		30.9	-
1,2 ins	99.8	-	99.8	-	99.7	-	99.8	-	99.8	-	99.6	-	>99.9	-	>99.9		99.9	-
[*mmmm*]	71.7	71.7	91.8	91.8	90.5	90.5	94.3	94.4	96.5	96.5	94.4	94.5	93.6	93.6	93.1	93.2	95.0	95.0
[*mmmr*]	9.7	9.7	3.2	3.0	3.5	3.4	2.2	2.0	1.1	1.1	2.5	2.2	2.6	2.4	2.5	2.3	1.9	1.9
[*rmmr*]	0.6	0.4	0.4	0.1	0.3	0.1	0.3	0.1	0.3	0.1	0.7	0.0	0.3	0.0	0.6	0.1	0.2	0.2
[*mmrr*]	9.0	9.3	2.6	2.8	3.1	3.2	1.7	1.9	1.0	1.1	1.3	1.7	2.0	2.2	1.8	2.1	1.6	1.6
[*mrmm*] +[*rmrr*]	2.0	2.1	0.3	0.5	0.5	0.6	0.3	0.4	0.2	0.3	0.2	0.7	0.1	0.4	0.3	0.6	0.1	0.1
[*mrmr*]	0.8	0.9	0.2	0.2	0.2	0.2	0.1	0.2	0.1	0.2	0.2	0.1	0.2	0.1	0.2	0.2	0.1	0.1
[*rrrr*]	0.6	0.4	0.1	0.1	0.2	0.1	0.1	0.1	0.1	0.1	0.2	0.0	0.1	0.0	0.2	0.1	0.1	0.1
[*mrrr*]	0.8	0.9	0.2	0.2	0.2	0.2	0.1	0.2	0.1	0.1	0.1	0.1	0.1	0.1	0.2	0.2	0.1	0.1
[*mrrm*]	4.8	4.6	1.3	1.4	1.5	1.6	0.8	0.9	0.5	0.5	0.5	0.8	1.0	1.1	1.0	1.0	0.7	0.7
total	100.0	100.0	100.0	100.0	100.0	100.0	100.0	100.0	100.0	100.0	100.1	100.0	100.0	100.0	99.9	100.0	99.8	99.8
RMS [c]	-	0.1542	-	0.1603	-	0.1001	-	0.1225	-	0.1080	-	0.3389	-	0.1649	-	0.2367	-	0.1069
a [d]		0.3263		0.2982		0.3938		0.2504		0.7681		0.1277		0.2546		0.5002		0.6657
b [d]		0.9415		0.9859		0.9839		0.9911		0.9976		0.9921		0.9888		0.9905		0.9923
k [d]		0.9940		0.9972		0.9965		0.9974		0.9929		0.9964		0.9982		0.9954		0.9970

[a] Experimental data; [b] DFT calculated data; ***a*** and ***b*** – the probabilities of stereoselective insertion on the open and crowded metallocene faces, respectively; ***k*** – the probability of site epimerization. [c] $RMS = ((\Sigma(I_{obs} - I_{calc})^2/9)^{0.5}$.

CONCLUSION

We have synthesized a new series of C_1-symmetric group 4 *ansa*-metallocene precursors incorporating substituted silylene-bridged {Cp/Ind} ligands. The main geometrical parameters (*e.g.*, Cp_{cent}–M and Ind_{cent}–M distances and Cp_{cent}–M–Ind_{cent} bite angles) within this series of complexes are quite similar; hence, the reason for the enhanced catalytic activity in complexes featuring one (**2c**) and two (**2d**, **3e**)-OMe groups can be reasonably ascribed to the sole presence of the π-donating substituent. These complexes, after activation with MAO, are highly active towards propylene under homogeneous conditions and give highly isotactic polypropylenes with high melting points. The corresponding silica-MAO-supported catalytic systems also afforded iPPs with high productivities, stereo- and regio-selectivities. Unexpectedly, we demonstrated experimentally that the presence of *i*Pr groups in the Cp moiety has a deleterious effect on the catalytic activity of the metallocene complexes, affording atactic oligomers with poor productivities. This inhibition might be caused by the formation of dormant zirconacyclic species and we anticipate that further investigations will help deciphering the mechanism at play. Identification of the stereocontrol mechanism and thermochemical data obtained through the computations in this study will be used to develop new more selective and performing metallocene systems.

ASSOCIATED CONTENT

Supporting information is available free of charge on the ACS Publications website at DOI:

Experimental section (general considerations, instruments, methods and measurements, synthetic and computational details), NMR spectra, Figures and Tables giving additional

characterization data. Crystallographic data for CCDC **2b-Zr**, **2d-Zr**, **2e-Zr**, **2f-Zr**, **2b-Hf**, **2d-Hf**, **2j-Zr** and **2k-Zr**.

AUTHOR INFORMATION

Notes

The authors declare no competing financial interests.

AKNOWLEDGMENTS

This work was financially supported by TotalEnergies (PhD grant to DT and ID, postdoctoral fellowship to MAP and SAD).

REFERENCES

[1] (a) Resconi, L.; Fritze, C. in *Polypropylene Handbook* (Ed.: Pasquini, N.), Hanser Publishers, Munich, 2005, pp 107–147. (b) Kaminsky, W. Discovery of Methylaluminoxane as Cocatalyst for Olefin Polymerization. *Macromolecules* **2012**, *45*, 3289–3297. (c) Fink, G.; Brintzinger, H. H. in *Metal-Catalysis in Industrial Organic Processes* (Eds. Chiusoli, G. P.; Maitlis, P. M.), Royal Society of Chemistry, Colchester, 2006, pp 218–254. (d) Razavi, A. Metallocene catalysts technology and environment. *C. R. Acad. Sci., Chem.* **2000**, *3*, 615–625.

[2] Ewen J. A. Mechanisms of Stereochemical Control in Propylene Polymerizations with Soluble Group 4B Metallocene/Methylalumoxane Catalysts. *J. Am. Chem. Soc.* **1984**, *106*, 6355-6364.

[3] Kaminsky, W.; Kulper, K.; Brintzinger, H. H.; Wild, F. R. W. P. Polymerization of Propene and Butene with a Chiral Zirconocene and Methylalumoxane as Cocatalyst. *Angew. Chem., Int. Ed. Engl.* **1985**, *24*, 507−508.

[4] (a) Resconi, L.; Cavallo, L.; Fait, A.; Piemonntesi, F. Selectivity in propene polymerization with metallocene catalysts. *Chem. Rev.* **2000**, *100*, 1253–1345. (b) Busico, V.; Cipullo, R. Microstructure of polypropylene *Prog. Polym. Sci.* **2001**, *26*, 443–533.

[5] (a) Kaminsky, W. Discovery of Methylaluminoxane as Cocatalyst for Olefin Polymerization. *Macromolecules* **2012**, *45*, 3289–3297. (b) Razavi, A. Metallocene catalysts technology and environment. *C. R. Acad. Sci., Chem.* **2000**, *3*, 615–625.

[6] Spaleck, W.; Kuber, F.; Winter, A.; Rohrmann, J.; Bachmann, B.; Antberg, M.; Dolle, V.; Paulus, E. F. The Influence of Aromatic Substituents on the Polymerization Behavior of Bridged Zirconocene Catalysts. *Organometallics* **1994**, *13*, 954−963.

[7] (a) Razavi, A.; Thewalt, U. Site selective ligand modification and tactic variation in polypropylene chains produced with metallocene catalysts. *Coord. Chem. Rev.* **2006**, *250*, 155–169. (b) Razavi, A.; Belia, V.; Baekelmans, D.; Slawinsky, M.; Sirol, S.; Peters, L.; Thewalt, U. Chain "stationary" insertion mechanism and production of isotactic polypropylene with C_1 symmetric catalyst systems. *Kinetics and Catalysis* **2006**, *47*, 257–267. (c) Boggioni, L.; Cornelio, M.; Losio, S.; Razavi, A.; Tritto, I. Propene Polymerization with C_1-Symmetric Fluorenyl-Metallocene Catalysts. *Polymers* **2017**, *9*, 581–598. (d) Kirillov, E.; Carpentier, J.-F. {Cyclopentadienyl/Fluorenyl}-Group 4 ansa-Metallocene Catalysts for Production of Tailor-Made Polyolefins. *Chem. Rec.* **2021**, *21*, 357−375.

[8] Ehm, C.; Vittoria, A.; Goryunov, G. P.; Kulyabin, P. S.; Budzelaar, P. H. M.; Voskoboynikov, A. Z.; Busico, V.; Uborsky, D. V.; Cipullo, R. Connection of

Stereoselectivity, Regioselectivity, and Molecular Weight Capability in *rac*-R′$_2$Si(2-Me-4-R-indenyl)$_2$ZrCl$_2$ Type Catalysts. *Macromolecules* **2018**, *51*, 8073−8083.

[9] Ehm, C.; Vittoria, A.; Goryunov, P. G.; Izmer, V. V.; Kononovich, S. D.; Samsonov, V. O.; Di Girolamo, R.; Budzelaar, H. M. P.; Voskoboynikov, Z. A.; Busico, V.; Uborsky, V. D.; Cipullo, R. An Integrated High Throughput Experimentation/Predictive QSAR Modeling Approach to *ansa*-Zirconocene Catalysts for Isotactic Polypropylene. *Polymers* **2020**, *12*, 1005.

[10] Deng, H.; Winkelbach, H.; Taeji, K.; Kaminsky, K.; Soga, K. Synthesis of High-Melting, Isotactic Polypropene with C_2- and C_1-Symmetrical Zirconocenes. *Macromolecules* **1996**, *29*, 6371–6376.

[11] Schöbel, A.; Herdtweck, E.; Parkinson, M.; Rieger, B. Ultra-Rigid Metallocenes for Highly Iso- and Regiospecific Polymerization of Propene: The Search for the Perfect Polypropylene Helix. *Chem. - Eur. J.* **2012**, *18*, 4174−4178.

[12] Nifant'ev, I. E.; Ivchenko, P. V.; Bagrov, V. V.; Churakov, A. V.; Mercandelli, P. 5-Methoxy-Substituted Zirconium Bis-indenyl *ansa*-Complexes: Synthesis, Structure, and Catalytic Activity in the Polymerization and Copolymerization of Alkenes, *Organometallics* **2012**, *31*, 4962−4970.

[13] Kulyabin, P. S.; Goryunov, G. P.; Sharikov, M. I.; Izmer, V. V.; Vittoria, A.; Budzelaar, P. H. M.; Busico, V.; Voskoboynikov, A. Z.; Ehm, C.; Cipullo, R.; Uborsky, D. V. *ansa*-Zirconocene Catalysts for Isotactic-Selective Propene Polymerization at High Temperature: A Long Story Finds a Happy Ending. *J. Am. Chem. Soc.* **2021**, *143*, 7641–7647.

[14] Spaleck, W.; Antberg, M.; Dolle, V.; Klein, R.; Rohrmann, J.; Winter, A. Stereorigid metallocenes: correlations between structure and behavior in homopolymerizations of propylene. *New J. Chem.* **1990**, *14*, 499–503.

[15] Mallin D. T.; Marvin D. Rausch, M. D.; Lin Y.-G.; Dong S.; Chien J. C. W. *rac*-[Ethylidene(1-η^5-tetramethylcyclopentadienyl)(1-η^5-indenyl)]dichlorotitanium and Its Homopolymerization of Propylene to Crystalline-Amorphous Block Thermoplastic Elastomers. *J. Am. Chem. Soc.* **1990**, *112*, 2030-2031.

[16] Collins, S.; Gauthier, W. J. Elastomeric Poly(propylene): Propagation Models and Relationship to Catalyst Structure. *Macromolecules* **1995**, *28*, 3779-3786.

[17] Miyake, S.; Okumura, Y.; Inazawa; S. Highly Isospecific Polymerization of Propylene with Unsymmetrical Metallocene Catalysts. *Macromolecules* **1995**, 28, 3074–3079.

[18] Lee, M. H.; Han, Y.; Kim, D-H.; Hwang, J. W.; Do, Y. Isospecific Propylene Polymerization by C_1-Symmetric $Me_2Si(C_5Me_4)$(2-R-Ind)MCl_2 (M = Ti, Zr) Complexes, *Organometallics* **2003**, *22*, 2790-2796.

[19] Fendrick, C. M.; Schertz, L. D.; Mintz, E. A.; Marks, T. J. Transition Metal Organometallics and ligands. *Inorg. Synth.* **1992**, *29*, 193–198.

[20] (a) Yoshida, T.; Koga, N.; Morokuma, K. A Combined ab Initio MO−MM Study on Isotacticity Control in Propylene Polymerization with Silylene-Bridged Group 4 Metallocenes.C2 Symmetrical and Asymmetrical Catalysts. *Organometallics* **1996**, *15*, 766–777. (b) Laine, A.; Coussens, B. B.; Hirvi, J. T.; Berthoud, A.; Friederichs, N.; Severn, J. R.; Linnolahti, M. Effect of Ligand Structure on Olefin Polymerization by a Metallocene/Borate Catalyst: A Computational Study. *Organometallics* **2015**, *34*, 2415–2421. (c) Kuklin, M. S.; Virkkunen, V.; Castro, P. M.; Resconi, L.; Linnolahti, M. Controlling the Microstructure of Isotactic Polypropene by C_2-Symmetric Zirconocene

Polymerization Catalysts: Influence of Alkyl Substituents on Regio- and Stereocontrol. *Eur. J. Inorg. Chem.* **2015**, 4420–4428.

[21] (a) Castro, L.; Kirillov, E.; Miserque, O.; Welle, A.; Haspeslagh, L.; Carpentier, J.-F.; Maron, L. Are Solvent and Dispersion Effects Crucial in Olefin Polymerization DFT Calculations? Some Insights from Propylene Coordination and Insertion Reactions with Group 3 and 4 Metallocenes. *ACS Catal.* **2015**, *5*, 416–425. (b) Castro, L.; Theurkauff, G.; Vantomme, A.; Welle, A.; Haspeslagh, L.; Brusson, J.-M.; Maron, L.; Carpentier, J.-F.; Kirillov, E. A Theoretical Outlook on the Stereoselectivity Origins of Isoselective Zirconocene Propylene Polymerization Catalysts *Chem. Eur. J.* **2018**, *24*, 10784–10792.

[22] Villaseñor, E.; Gutierrez-Gonzalez, R.; Carrillo-Hermosilla, F.; Fernández-Galán, R.; López-Solera, I.; Fernández-Pacheco, A. R.; Antiñolo, A. Neutral Dimethylzirconocene Complexes as Initiators for the Ring-Opening Polymerization of ϵ-Caprolactone. *Eur. J. Inorg. Chem.* **2013**, *13*, 1184–1196.

[23] Lee, M. H.; Han, Y.; Kim, D.-H.; Hwang, J. W.; Do, Y. Isospecific Propylene Polymerization by C1-Symmetric $Me_2Si(C_5Me_4)$(2-R-Ind)MCl_2 (M = Ti, Zr) Complexes. *Organometallics* **2003**, *22*, 2790–2796.

[24] Friederichs, N. H.; Vittoria, A.; Cipullo, R.; Busico, V.; Borisov, I.; Guzeev, B. A.; Mladentsev, D. Y.; Sharikov, M. I.; Uborsky, D.; Voskoboynikov, A.; Coen, H. (to Sabic Global Technologies B.V.) *PCT Int. Appl.* WO 18/058630, **2018**.

[25] Shannon, R. D. Revised Effective Ionic Radii and Systematic Studies of Interatomic Distances in Halides and Chalcogenides. *Acta Cryst.* **1976**, *A32*, 751–767.

[26] Each polymerization experiment was repeated independently twice, revealing good reproducibility in terms of productivity (polymer yield) as well as T_m of the isolated polymer.

[27] Izmer, V. V.; Lebedev, A. Y.; Kononovich, D. S.; Borisov, I. S.; Kulyabin, P. S.; Goryunov, G. P.; Uborsky, D. V.; Canich, J. A. M.; Voskoboynikov, A. Z. *ansa*-Metallocenes Bearing 4-(*N*-Azolyl)-2-methylindenyl and Related Ligands: Development of Highly Isoselective Catalysts for Propene Polymerization at Higher Temperatures. *Organometallics* **2019**, *38*, 4645–4657.

[28] McGovern, G. P.; Hung-Low, F.; Tye, J. W.; Bradley, C. A. Synthesis and Reactivity Studies of Benzo-Substituted Bis(Indenyl) Iron and Zirconium Complexes: The Difference a Methyl Group Can Make. *Organometallics* **2012**, *31*, 3865–3879.

[29] Ewen, J. A.; Haspeslagh, L.; Atwood, J. L.; Zhang, H. Crystal structures and stereospecific propylene polymerizations with chiral hafnium metallocene catalysts, J. Am. Chem. Soc. **1987**, *109*, 6544.

[30] Rieger, B.; Troll, C. Ultrahigh Molecular Weight Polypropene Elastomers by High Activity "Dual-Side" Hafnocene Catalysts. *Macromolecules* **2002,** *35,* 5742-5743.

[31] Machat, M. R.; Fischer, A.; Schmitz, D.; Vöst, M.; Drees, M.; Jandl, C.; Pöthig, A.; Casati, N. P. M.; Scherer, W.; Rieger, B. Behind the Scenes of Group 4 Metallocene Catalysis: Examination of the Metal−Carbon Bond. *Organometallics* **2018**, *37*, 2690−2705.

[32] Busico, V.; Cipullo, R.; Pellecchia, R.; Talarico, G.; Razavi, A. Hafnocenes and MAO: Beware of Trimethylaluminum! *Macromolecules* **2009**, *42*, 1789-1791.

[33] Ehm, C.; Vittoria, A.; Goryunov, G. P.; Izmer, V. V.; Kononovich, D. S.; Kulyabin, P. S.; Di Girolamo, R.; Budzelaar, P. H. M.; Voskoboynikov, A. Z.; Busico, V.; Uborsky, D. V.; Cipullo, R. A Systematic Study of the Temperature-Induced Performance Decline of *ansa*-Metallocenes for iPP. *Macromolecules* **2020**, *53*, 9325−9336.

[34] Santoro, O.; Piola, L.; Cabe, K. Mc; Lhost, O.; Den Dauw, K.; Vantomme, A.; Welle, A.; Maron, L.; Carpentier, J.-F.; Kirillov, E. Long-Chain Branched Polyethylene via

Coordinative Tandem Insertion and Chain-Transfer Polymerization Using *rac*-{EBTHI}$ZrCl_2$/MAO/Al-alkenyl Combinations: An Experimental and Theoretical Study, *Macromolecules* **2020**, *53*, 8847–8857.

[35] (a) Farina, M.; Di Silvestro, G.; Sozzani, P. Hemitactic Polymers *Prog. Polym. Sci.* **1991**, *16*, 219–238. (b) Farina, M.; Terragni, A. On the syndiotactic polymerization mechanism using metallocene catalysts. *Makromol. Chem., Rapid Commun.* **1993**, *14*, 791–798. (c) Farina, M.; Di Silvestro, G.; Sozzani, P. Hemiisotactic polypropylene: a key point in the elucidation of the polymerization mechanism with metallocene catalysts. *Macromolecules* **1993**, *26*, 946–950. (d) Farina, M.; Di Silvestro, G.; Terragni, A. A stereochemical and statistical analysis of metallocene-promoted polymerization. *Macromol. Chem. Phys.* **1995**, *196*, 353–367. (e) Di Silvestro, G.; Sozzani, P.; Terragni, A. Polymerization of propene with enantiomorphic site catalysts, 1. A statistical analysis. *Macromol. Chem. Phys.* **1996**, *197*, 3209–3228.